MREIT Conductivity Imaging of Pneumonic Canine Lungs: Preliminary Post-mortem Study

Hyung Joong Kim[1], Young Tae Kim[1], Woo Chul Jeong[1], Atul S. Minhas[1], Tae Hwi Lee[1], Chae Young Lim[2], Hee Myung Park[2], O Jung Kwon[3], and Eung Je Woo[1]

[1]*Department of Biomedical Engineering, Kyung Hee University, Gyeonggi-do, Korea.*
[2]*BK21 Basic & Diagnostic Veterinary Specialist Program for Animal Diseases and Department of Veterinary Internal Medicine, Konkuk University, Seoul, Korea*
[3]*Division of Pulmonary and Critical Care Medicine, Department of Medicine, Samsung Medical Center, Sungkyunkwan University School of Medicine, Seoul, Korea*
(Received October 12, 2009. Accepted March 17, 2010)

Abstract

In magnetic resonance electrical impedance tomography (MREIT), a current-injection MR imaging method is adopted to produce a cross-sectional image of an electrical conductivity distribution in addition to MR images. The purpose of this study was to test the feasibility of MREIT for differentiating the canine lung parenchyma without and with pneumonia. Three normal healthy beagles and two mixed breed dogs with pneumonia were used. After attaching electrodes around the chest, we placed the dog inside our MR scanner. We injected as much as 30 mA current in a form of short pulses into the chest region. Reconstructed conductivity images of normal canine lungs exhibit a peculiar pattern of a relatively coarse salt and pepper noise. On the contrary, conductivity images of pneumonic canine lungs show significantly enhanced contrast of the lesions while the corresponding MR images show a little bit of contrast in the middle and caudal lung parenchyma due to the accumulation of pleural fluid. This preliminary study indicates that MREIT imaging of the chest may deliver unique new diagnostic information.

Key words : magnetic resonance electrical impedance tomography, conductivity image, pneumonia, lung parenchyma

I. INTRODUCTION

MR imaging of the lung parenchyma is known to be troublesome because of physical and physiological factors such as low proton density, susceptibility effects, respiratory movements, cardiac and vascular pulsations [1, 2]. There are several MR strategies to overcome these problems and some are based on standard ^{1}H MRI aimed at increasing the SNR of lung parenchyma [3-5]. Since the low SNR of lung parenchyma may give a contrast between normal and abnormal tissues, lung imaging is still one of the most challenging organs in MR imaging area.

Magnetic resonance electrical impedance tomography (MREIT) is a new bio-imaging modality providing cross-sectional conductivity images from measurements of internal magnetic flux densities produced by externally injected currents [6-12]. MRI scanner is used as a tool to measure the induced magnetic flux density inside an imaging object. Recent postmortem and *in vivo* animal experiments demonstrated its feasibility by showing conductivity images with meaningful contrast among different biological tissues [13-15]. Numerous animal studies focusing on organs of interest in terms of their conductivity contrast must precede clinical trials.

In this study, we test the potential of the MREIT technique as a new clinically useful bio-imaging modality for differentiating the lung parenchyma without and with pneumonia. Describing the imaging method, we will show cross-sectional conductivity images of canine chests without and with pneumonia. We expect that this kind of postmortem animal imaging can provide conductivity information on tissues *in situ* to be utilized in numerous modeling studies.

Corresponding Author : Eung Je Woo
Department of Biomedical Engineering, College of Electronics and Information, Kyung Hee Univ.
1 Seochun, Giheung, Yongin, Gyeonggi, 446-701, Korea
Tel : +82-31-201-2538 / Fax : +82-31-201-2378
E-mail : ejwoo@khu.ac.kr
This work was supported by the SRC/ERC program (R11-2002-103) of MEST/NRF.

II. MATERIALS AND METHODS

A. Animals

Three healthy laboratory beagles (females, 5-12 months old) were used as a control group. All of them were healthy without a signs of neurological problems on physical examination. Two mixed breed dogs (females, 5 months old) were taken to a veterinarian due to mucopurulent oculonasal discharge, severe moist coughing, retching, and signs of pulmonary disease. Physical examinations revealed pale mucous membranes, enlarged mandibular lymph nodes, and fever (body temperatures was 40℃ for dog 1, 40.2℃ for dog 2). The complete blood count showed lymphopenia and neutrophilic leukocytosis. Thoracic radiographs revealed a mixed pattern of increased alveolar and interstitial densities, compatible with pneumonia. Conjunctival swabs tested positive for canine distemper virus (CDV) by polymerase chain reaction. Based on these findings, pneumonia secondary to CDV was strongly suspected.

At necropsy after each imaging experiment, the entire lungs of the two dogs were compact, dark red, and edematous, with slight serous effusion in the pleural cavity. Histologically, the lung parenchyma showed a severe diffuse acute fibrinous pneumonia with an accompanying exudation of neutrophils and macrophages into the alveoli.

B. Animal Preparation for Imaging

To prevent dribbling, we injected 0.1 mg/kg of atrophine sulfate. Ten minutes later, we anesthetized the dog with intramuscular injection of 0.2 ml/kg Tiletamine and Zolazepam (Zoletil 50, Virbac, France). Twenty minutes later, we sacrificed it with an intravenous injection of 80 mg/kg (Entobar, Hanrim Pharmacy, Korea). After clipping and shaving the hair at the chest region, we rubbed the region of electrode attachment using a skin preparation gel (D.O. Weaver and Co., USA). This procedure was approved by the Institutional Animal Care and Use Committee (IACUC) of Konkuk University, Seoul, Korea.

C. Imaging Experiment

We attached four carbon-hydrogel electrodes (HUREV Co. Ltd., Korea) around the chest (Fig. 1). The size of each electrode was $80\times80\times5.76$ mm^3. We placed the animal inside the bore of our 3T MRI scanner (Magnum 3, Medinus Co. Ltd., Korea). We injected currents in two mutually orthogonal directions between two pairs of electrodes facing each other. The injection current amplitude ranged from 30 to 35 mA. We used the injection current nonlinear encoding (ICNE) pulse sequence [16]. The imaging parameters were as follows: TR/TE = 1000/30 ms, FOV = 240×240 mm^2, matrix size = 128×128, slice thickness = 5 mm, number of slices = 8, NEX = 24 and total imaging time = 200 min.

D. Conductivity Image Reconstruction

We used CoReHA (conductivity reconstructor using harmonic algorithms), which is an integrated software package for MREIT [15, 17, 18]. We used the single-step harmonic B_z algorithm implemented in CoReHA for multi-slice conductivity image reconstructions [19]. All conductivity images presented in this paper should be interpreted as scaled conductivity images providing only contrast information.

III. RESULTS

A. Normal Canine Lung

Figure 2 shows chest images obtained from a normal dog. The lung parenchyma appears as dark regions in the MR magnitude image due to MR signal void there. In the reconstructed conductivity image, lung regions turn out to be noisy [20, 21]. The regions exhibit a peculiar pattern of a relatively coarse salt and pepper noise. Outside the regions, the conductivity image reveals contrasts among the heart, thoracic longissimus muscle, and thoracic wall.

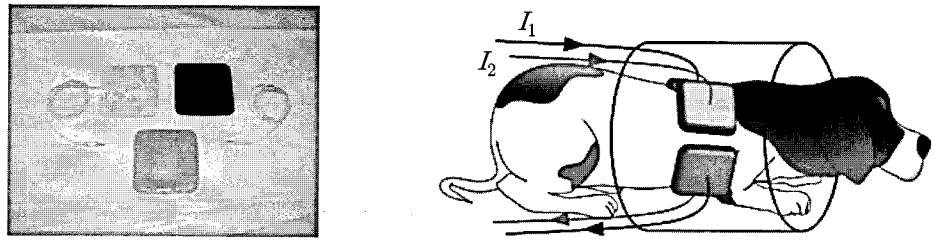

Fig. 1. (a) Carbon-hydrogel electrodes for current injection and (b) MREIT imaging setup inside the bore.

B. Pneumonic Canine Lung

Figure 3 shows chest images obtained from the first dog with pneumonia. The MR magnitude image shows somewhat increased contrast in the middle and caudal lung parenchyma due to the accumulation of pleural fluid. On the contrary, the corresponding conductivity image shows a significantly increased contrast. Figure 4 shows results from the second dog with pneumonia. Conductivity images show increased conductivity contrasts in the left middle and caudal lung parenchyma. Especially, the increased conductivity contrast in the right middle lung parenchyma provides valuable information which is not available from MR magnitude images. Figure 5 shows multi-slice MR magnitude and conductivity images from normal and pneumonic canine chests.

Ⅳ. DISCUSSION AND CONCLUSION

MREIT has now reached the stage of animal and human experiments. To support its clinical significance, we should demonstrate that the conductivity image provides meaningful diagnostic information that is not available from other imaging modalities. In this preliminary study, we found that reconstructed conductivity images from pneumonic canine lungs show a significantly increased conductivity contrast, which are much larger than a contrast change of the same

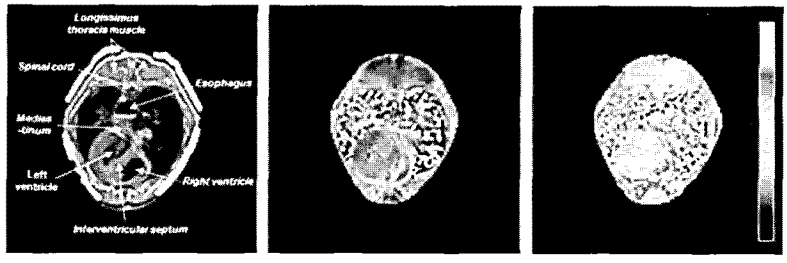

Fig. 2. Chest images of a normal dog. (a) MR magnitude image, (b) reconstructed conductivity image, and (c) color-coded conductivity image. Conductivity image inside the lungs show a pattern of spurious spike noise due to the MR signal void there.

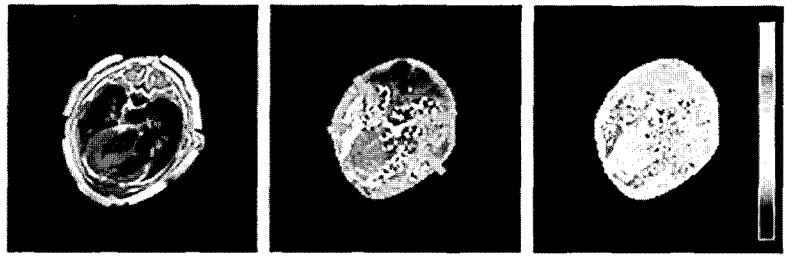

Fig. 3. Chest images of the first dog with pneumonia. (a) MR magnitude image, (b) reconstructed conductivity image, and (c) color-coded conductivity image. In the middle and caudal lung of both lobes (arrows), the conductivity image shows a significantly increased contrast, which is not apparent in the corresponding MR image.

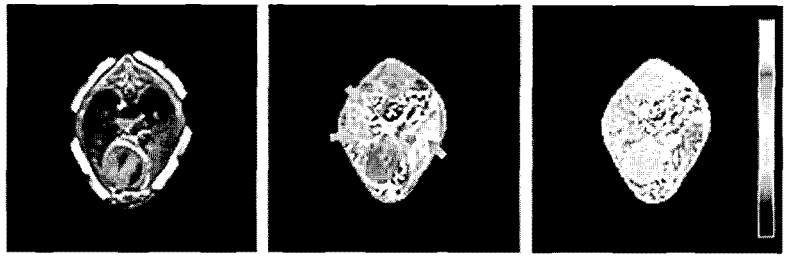

Fig. 4. Chest images of the second dog with pneumonia. (a) MR magnitude image, (b) reconstructed conductivity image, and (c) color-coded conductivity image. In the right middle and caudal lung lobes (arrows), the conductivity image shows a much higher contrast compared with the corresponding MR image.

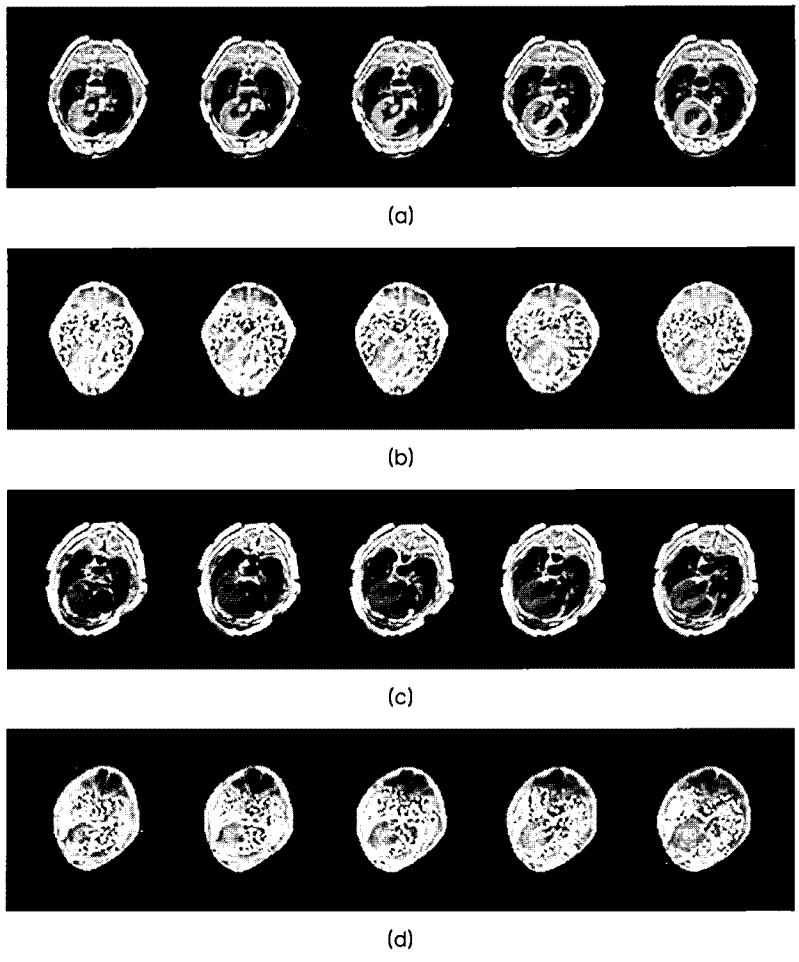

Fig. 5. Multi-slice chest images of a normal dog: (a) MR magnitude and (b) conductivity images. (c) and (d) are MR magnitude and conductivity images of the first dog with pneumonia. Conductivity images in (b) and (d) show unique regional information about the lung parenchyma.

lungs in conventional MR images. This implies that pneumonia is accompanied by a significant increase of local conductivity values.

All conductivity images presented in this paper should be interpreted as equivalent isotropic scaled conductivity images providing only conductivity-based contrast information. Interpretation of these images should be pursued in future work [18]. The contrast information in our conductivity images depend on the signal intensity and noise standard deviation in B_z images. The B_z noise is inversely proportional to the SNR of magnitude image and current injection duration [21]. Together with the somewhat increased MR signals in the lung parenchyma, the current injection duration enabled substantial conductivity contrast in that region due to the accumulation of pleural fluid.

The present gold standard for diagnosing pneumonia is the chest radiography. Infiltrates in the lungs, as seen on the radiograph, usually confirms the diagnosis. However, since the chest radiograph is frequently found to be negative in patients suspected of having pneumonia [22], computed tomography (CT) plays an increasingly important role in cases where radiographic findings are equivocal [23, 24].

MR imaging of the lung parenchyma has long been neglected because of the unique intrinsic difficulties such as signal loss due to cardiac pulsation and respiration, susceptibility artifacts caused by multiple air-tissue interfaces, and low proton density [1, 2]. Even though there are several MR strategies to overcome these problems by increasing the signal-to-noise ratio (SNR) [3-5], lungs usually appear as low contrast regions in MR images.

Equipped with a different contrast mechanism, MREIT imaging of the chest could be supplementary to the conventional MR imaging. We speculate that MREIT could be advantageous in distinguish lung diseases such as pneumonia, edema, and pulmonary tuberculosis based on conductivity changes associated with them.

We suggest MREIT as a new lung imaging method supplementing conventional chest MR imaging techniques. Imaging experiments of animal models with several lung diseases must be undertaken. These experimental validation studies demand technical progresses in terms of specialized MREIT pulse sequence and RF coil. MREIT must be accompanied by recent technical advancement in general MRI technology including fast imaging methods and ECG gating.

REFERENCES

[1] C. Leutner, H. Schild, "MRI of the lung parenchyma", *RoFo*, vol. 173, pp. 168-175, 2001.

[2] C.J. Bergin, D.C. Noll, J.M. Pauly, G.H. Glover, A. Macovski, "MR imaging of lung parenchyma: a solution to susceptibility", *Radiology*, vol. 183, pp. 673-676, 1992.

[3] J.R. Mayo, A. MacKay, N.L. Muller, "MR imaging of the lungs: value of short TE spin-echo pulse sequences", *Am. J. Roentgenol.*, vol. 159, pp. 951-956, 1992.

[4] D.L. Levin, Q. Chen, M. Zhang, R.R. Edelman, H. Hatabu, "Evaluation of regional pulmonary perfusion using ultrafast magnetic resonance imaging", *Magn. Reson. Med.*, vol. 46, pp. 166-171, 2001.

[5] V.M. Mai, J. Knight-Scott, R.R. Edelman, Q. Chen, S. Keilholz-George, S.S. Berr, "1H magnetic resonance imaging of human lung using inversion recovery turbo spin echo", *J. Magn. Reson. Imaging.*, vol. 11, pp. 616-621, 2000.

[6] G.C. Scott, M.L.G. Joy, R.L. Armstrong, and R.M. Henkelman, "Measurement of nonuniform current density by magnetic resonance", *IEEE Trans. Med. Imag.*, vol. 10, pp. 362-374, 1991.

[7] N. Zhang, *Electrical Impedance Tomography based on Current Density Imaging*, Toronto, Canada: MS Thesis, Dept. of Elec. Eng, 1992.

[8] E.J. Woo, S.Y. Lee, and C.W. Mun, "Impedance tomography using internal current density distribution measured by nuclear magnetic resonance", *SPIE*, vol. 2299, pp. 377-385, 1994.

[9] O. Birgul, Y.Z. Ider, "Electrical impedance tomography using the magnetic field generated by injected currents", *Proc. 18th Ann. Int. Conf. IEEE EMBS*, pp. 784-785, 1996.

[10] Y.Z. Ider, and O. Birgul, "Use of the magnetic field generated by the internal distribution of injected currents for electrical impedance tomography (MR-EIT)", *Elektrik*, vol. 6, pp. 215-225, 1998.

[11] O. Kwon, E.J. Woo, J.R. Yoon, and J.K. Seo, "Magnetic resonance electrical impedance tomography (MREIT): simulation study of J-substitution algorithm", *IEEE Trans. Biomed. Eng.*, vol. 49, pp. 160-167, 2002.

[12] E.J. Woo, and J.K. Seo, "Magnetic resonance electrical impedance tomography (MREIT) for high-resolution conductivity imaging", *Physiol. Meas.*, vol. 29, pp. R1-26, 2008.

[13] H.J. Kim, B.I. Lee, Y. Cho, Y.T. Kim, B.T. Kang, H.M. Park, S.Y. Lee, J.K. Seo, and E.J. Woo, "Conductivity imaging of canine brain using a 3 T MREIT system: postmortem experiments", *Physiol. Meas.*, vol. 28, pp. 1341-1353, 2007.

[14] H.J. Kim, T.I. Oh, Y.T. Kim, B.I. Lee, E.J. Woo, J.K. Seo, S.Y. Lee, O. Kwon, C. Park, B.T. Kang, and H.M. Park, "*In vivo* electrical conductivity imaging of a canine brain using a 3T MREIT system", *Physiol. Meas.*, vol. 29, pp. 1145-1155, 2008.

[15] K. Jeon, A.S. Minhas, Y.T. Kim, W.C. Jeong, H.J. Kim, B.T. Kang, H.M. Park, C.O. Lee, J.K. Seo, E.J. Woo, "MREIT conductivity imaging of postmortem canine abdomen using CoReHA", *Physiol. Meas.*, vol. 30, pp. 957-966, 2009.

[16] C. Park, B.I. Lee, O. Kwon, and E.J. Woo, "Measurement of induced magnetic flux density using injection current nonlinear encoding (ICNE) in MREIT", *Physiol. Meas.*, vol. 28, pp. 117-127, 2007.

[17] IIRC, CoReHA 1.0 Installation and User's Guide. Available via http://iirc.khu.ac.kr., 2009.

[18] K. Jeon, H.J. Kim, C.O. Lee, E.J. Woo, J.K. Seo, "CoReHA: conductivity reconstructor using harmonic algorithms for magnetic resonance electrical impedance tomography (MREIT). *J. Biomed. Eng. Res.* at press.

[19] J.K. Seo, S.W. Kim, S. Kim, J.J. Liu, E.J. Woo, K. Jeon, and C.O. Lee, "Local harmonic B_z algorithm with domain decomposition in MREIT: computer simulation study", *IEEE Trans. Med. Imag.*, vol. 27, pp. 1754-1761, 2008.

[20] B.I. Lee, S.H. Oh, E.J. Woo, S.Y. Lee, M.H. Cho, O. Kwon, J.K. Seo, J.Y. Lee, and W.S. Baek, "Three-dimensional forward solver and its performance analysis in magnetic resonance electrical impedance tomography (MREIT) using recessed electrodes", *Phys. Med. Biol.*, vol. 48, pp. 1971-1986, 2003.

[21] R. Sadleir, S. Grant, S.U. Zhang, B.I. Lee, H.C. Pyo, S.H. Oh, C. Park, E.J. Woo, S.Y. Lee, O. Kwon, and J.K. Seo, "Noise analysis in MREIT at 3 and 11 Tesla field strength", *Physiol. Meas.*, vol. 26, pp. 875-884, 2005.

[22] T.R. Wilkins, R.L. Wilkins, "Clinical and radiographic evidence of pneumonia", *Radiol. Technol.*, vol. 77, pp. 106-110, 2005.

[23] H.U. Kauczor, K.F. Kreitner, "MRI of the pulmonary parenchyma", *Eur. Radiol.*, vol. 9, pp. 1755-1764, 1999.

[24] G. Lutterbey, J. Gieseke, M. von Falkenhausen, N. Morakkabati, H. Schild, "Lung MRI at 3.0T: a comparison of helical CT and high-field MRI in the detection of diffuse lung disease", *Eur. Radiol.*, vol. 15, pp. 324-328, 2005.